

Magneto-Rotational Transport in the Early Sun

Kristen Menou

*Department of Astronomy, Columbia University, 550 West 120th Street, New York, NY
10027, USA*

and

Joël Le Mer

*Ecole Polytechnique, Route de Saclay, 91128 Palaiseau, France &
Department of Astronomy, Columbia University, 550 West 120th Street, New York, NY
10027, USA*

ABSTRACT

Angular momentum transport must have occurred in the Sun’s radiative zone to explain its current solid body rotation. We survey the stability of the early Sun’s radiative zone with respect to diffusive rotational instabilities, for a variety of plausible past configurations. We find that the (faster rotating) early Sun was prone to rotational instabilities even if only weak levels of radial differential rotation were present, while the current Sun is not. Stability domains are determined by approximate balance between dynamical and diffusive timescales, allowing generalizations to other stellar contexts. Depending on the strength and geometry of the weak magnetic field present, the fastest growing unstable mode can be hydrodynamic or magneto-hydrodynamic (MHD) in nature. Our results suggest that diffusive MHD modes may be more efficient at transporting angular momentum than their hydrodynamic (“Goldreich-Schubert-Fricke”) counterparts because the minimum spatial scale required for magnetic tension to be destabilizing limits the otherwise very small scales favored by double-diffusive instabilities. Diffusive magneto-rotational instabilities are thus attractive candidates for angular momentum transport in the early Sun’s radiative zone.

Subject headings: hydrodynamics – instabilities – stars: rotation – Sun: rotation – turbulence

1. Introduction

The Sun’s internal structure, which has been probed extensively with seismological techniques (Thompson et al. 2003), is a unique laboratory for the study of fluid dynamical processes on astronomical scales. In this context, it is rather significant that the physical process at the origin of the solid body rotation in the Sun’s radiative zone has not yet been unambiguously identified. By analogy with young Sun-like stars, it is believed that the young Sun was rotating faster than it currently is (by a factor up to ~ 50) and that it was subsequently spun down by magnetic torques associated with the solar wind (see, e.g., Sofia et al. 1991 for a review). Although details are missing, the end result of this rotational evolution should be a differentially rotating interior, with a faster rotating core. Consequently, the well-established solid body rotation in the current Sun’s radiative zone is evidence that an efficient angular momentum transport mechanism has operated in the past. It is also tempting to associate this transport mechanism with “deep,” large-scale mixing of elements (below the convection zone), as required to explain the much depleted lithium abundance at the solar photosphere (e.g. Chaboyer, Demarque & Pinsonneault 1995a, 1995b).

The motivation to identify a successful transport mechanism for the Sun’s radiative zone goes in fact much beyond the Sun itself, as this mechanism is likely to also have consequences for the evolution of rotating massive stars (e.g., Woosley, Heger & Weaver 2002), the spin of newly-formed compact objects resulting from this evolution (e.g. Ott et al. 2006) and possibly the origin of gamma-ray bursts (e.g. MacFadyen & Woosley 1999). The mechanism could be operating in the radiative zones of all kinds of stars or only at some stages of their evolution, but until its nature is known, it is difficult to be more specific.

Efforts to understand transport in stellar radiative zones are not new (e.g. Tassoul 1978). It was clear early on that the microscopic kinematic viscosity in the Sun, ν_{\odot} , would not be sufficient to reduce any global scale differential rotation present, since the corresponding viscous timescale,

$$\tau_{\text{vis}} \simeq \frac{R_{\odot}^2}{\nu_{\odot}} \sim 10^{12-13} \text{ years}, \quad (1)$$

is prohibitively long (e.g. Goldreich & Schubert 1967). To explain the solid body rotation of the solar radiative zone which was later revealed by helioseismology, another process must have been operating.

Several candidate mechanisms have indeed been proposed. The list includes the so-called GSF instability (Goldreich & Schubert 1967; Fricke 1968), the “secular hydrodynamical shear instability” (Zahn 1974) and internal gravity waves (e.g. Kumar & Quataert 1997; Talon & Zahn 1998; Talon, Kumar & Zahn 2002; Charbonnel & Talon 2005). No consensus has been

reached yet as to which of these mechanisms, if any, provides a satisfactory answer to the current state of solid body rotation. The GSF instability alone is not expected to bring a radiative zone to a state of solid body rotation because its marginal stability conditions still allow for substantial differential rotation across cylindrical radii (Goldreich & Schubert 1967). The existence of the secular shear instability has not been rigorously established but rather suggested on the basis of heuristic arguments (Zahn 1974; Schatzman 1991), which makes it a difficult subject of detailed study. The efficiency of internal gravity waves at transporting angular momentum has been much debated in the literature (e.g. Press 1981; Talon & Zahn 1998; Talon, Kumar & Zahn 2002; Charbonnel & Talon 2005; Rogers & Glatzmeier 2005, 2006). It is also a priori unclear whether waves, which by nature transport energy and momentum but not the fluid itself, can achieve a sufficient level of deep mixing of elements such as lithium, whose depleted photospheric abundance is arguably more easily attributed to instabilities and turbulent mixing (but see Garcia-Lopez & Spruit 1991; Schatzman 1993; Charbonnel & Talon 2005 for a different view).

In recent years, magnetic fields have taken central stage in this discussion (e.g. Turck-Chieze et al. 2005). The role of a magnetic field has been discussed in relation to that of internal gravity waves (e.g. Mathis & Zahn 2005; Rashba, Semikoz & Valle 2005). Solar evolutionary models which account for rotation and effects attributed to magnetic fields have been presented by Eggenberger, Maeder & Meynet (2006). Spruit (2002) and Braithwaite & Spruit (2006) have discussed the possibility of growing an azimuthal magnetic field via stretching by differential rotation, followed by an instability, in stably stratified radiative zones. Finally, Menou, Balbus & Spruit (2004) have generalized the diffusive stability analysis of GSF to the case when a weak magnetic field is present in the radiative zone. These diffusive rotational instabilities and their potential role for the early Sun’s radiative zone are our main subjects of interest here.

The usual difficulty one faces when invoking fluid instabilities in stellar radiative zones is that the strong radial thermal stratification present stabilizes the fluid against a wide variety of (adiabatic) perturbations. This is the case for rotational instabilities in particular, even if strong radial differential rotation (across spherical shells)¹ is present. For instance, one verifies readily that, for any reasonable amount of imposed radial differential rotation, the current Sun’s radiative zone would be stable according to both the general Solberg-Høiland

¹Any radiative zone with negative differential rotation within a spherical shell ($\partial \ln \Omega / \partial \theta < 0$) is subject to the standard magneto-rotational instability because perturbations tangential to the spherical shell are blind to the radial stratification, as shown by Balbus & Hawley (1994). Here, we are focusing exclusively on the more challenging, “orthogonal” situation where negative differential rotation exists across spherical shells ($\partial \ln \Omega / \partial \ln r < 0$; see Menou et al. 2004 for a discussion).

adiabatic criteria (e.g. Tassoul 1978) and their generalization to weakly-magnetized fluids (Balbus 1995).

A way around this difficulty has been proposed by Goldreich & Schubert (1967) and Fricke (1968), who have shown that rotational instabilities can still exist, provided perturbed fluid elements are allowed to exchange heat with their environment much faster than they exchange momentum. For such (diabatic) perturbations, the stabilizing role of thermal stratification is effectively neutralized when the perturbed fluid element reaches thermal equilibrium with its environment while its original momentum remains largely unchanged. In the solar interior, radiative heat diffusion is indeed orders of magnitude faster than viscous diffusion of momentum, thus motivating the double-diffusive analysis of Goldreich & Schubert and Fricke (hereafter GSF altogether). The basic double-diffusive mechanism invoked in these instabilities is related to that of “salt-finger” instabilities operating in the Earth’s oceans, except that the destabilizing salinity stratification is replaced here by a destabilizing profile of angular momentum.

In Menou et al. (2004), we studied numerically the stability of the current Sun’s radiative zone to diffusive magneto-rotational instabilities under a variety of imposed rates of radial differential rotation. It was found that the Sun is relatively stable, unless a fairly substantial rate of negative differential rotation is imposed. However, as we alluded before, this is probably not the right question to ask because angular momentum transport in the Sun’s radiative zone must have occurred in the past, when it was rotating faster. One would generally expect this faster rotation to be favorable to rotational instabilities. Therefore, we reconsider the stability of the radiative zone of the (faster rotating, early) Sun for various plausible rates of radial differential rotation. We do find that, if the early Sun was rotating at least a few times faster than it currently is, it was indeed much more prone to diffusive hydro- and magneto-rotational instabilities.

We describe our method of solution in §2. In §3, we present the results of our detailed stability survey for the early Sun’s radiative zone. In §4 we summarize key results, discuss some of their consequences and possible extensions of this work.

2. Method

Our analysis is entirely based on a local, linear axisymmetric stability analysis of differential rotation in a weakly-magnetized, stably-stratified fluid. We recall the dispersion relation obeyed by axisymmetric modes in a general context in §2.1. The choice of various physical parameters of importance in the dispersion relation for the early Sun is described

in §2.2. We then describe how we obtained numerical solutions of the dispersion relation in §2.3. In §2.4, we discuss the issue of the efficiency of momentum transport, that we estimate (or rather extrapolate) from fastest growing linear mode properties. Our basic analysis follows closely that presented in Menou et al. (2004), where additional details on the method can be found.

2.1. Dispersion Relation

The dispersion relation was derived in cylindrical coordinates, (R, ϕ, Z) , but we will later switch to spherical coordinates, (r, θ, ϕ) , for convenience. Axisymmetric Eulerian perturbations with a WKB space-time dependence $\exp[i(\mathbf{k} \cdot \mathbf{r} - \omega t)]$, where $\mathbf{k} = (k_R, 0, k_Z) = (k_r, k_\theta, 0)$ are considered. Starting from the set of MHD equations (continuity, momentum, induction, energy) that include the effects of viscosity, resistivity and heat conduction,

$$\frac{\partial \rho}{\partial t} + \nabla \cdot (\rho \mathbf{v}) = 0, \quad (2)$$

$$\begin{aligned} \rho \frac{\partial \mathbf{v}}{\partial t} + (\rho \mathbf{v} \cdot \nabla) \mathbf{v} &= -\nabla \left(P + \frac{B^2}{8\pi} \right) - \rho \nabla \Phi \\ &+ \left(\frac{\mathbf{B}}{4\pi} \cdot \nabla \right) \mathbf{B} + \mu \left(\nabla^2 \mathbf{v} + \frac{1}{3} \nabla (\nabla \cdot \mathbf{v}) \right), \end{aligned} \quad (3)$$

$$\frac{\partial \mathbf{B}}{\partial t} = \nabla \times (\mathbf{v} \times \mathbf{B}) - \eta \nabla \times (\nabla \times \mathbf{B}), \quad (4)$$

$$\frac{1}{(\gamma - 1)} P \frac{d \ln P \rho^{-\gamma}}{dt} = \chi \nabla^2 T, \quad (5)$$

one derives, under the Boussinesq approximation and ignoring self-gravity, the following fifth-order dispersion relation for local, axisymmetric, multi-diffusive modes,

$$\begin{aligned} &\tilde{\omega}_{b+v}^4 \omega_e \frac{k^2}{k_Z^2} + \tilde{\omega}_{b+v}^2 \omega_b \left[\frac{1}{\gamma \rho} (\mathcal{D}P) \mathcal{D} \ln P \rho^{-\gamma} \right] \\ &+ \tilde{\omega}_b^2 \omega_e \left[\frac{1}{R^3} \mathcal{D}(R^4 \Omega^2) \right] - 4\Omega^2 (\mathbf{k} \cdot \mathbf{v}_A)^2 \omega_e = 0, \end{aligned} \quad (6)$$

where

$$\begin{aligned} \mathbf{v}_A &= \mathbf{B}/\sqrt{4\pi\rho}, & k^2 &= k_R^2 + k_Z^2, \\ \tilde{\omega}_{b+v}^2 &= \omega_b\omega_v - (\mathbf{k} \cdot \mathbf{v}_A)^2, & \tilde{\omega}_b^2 &= \omega_b^2 - (\mathbf{k} \cdot \mathbf{v}_A)^2, \\ \omega_b &= \omega + i\eta k^2, & \omega_v &= \omega + i\nu k^2, \\ \omega_e &= \omega + \frac{\gamma - 1}{\gamma} \frac{iT}{P} \chi k^2, & \mathcal{D} &\equiv \left(\frac{k_R}{k_Z} \frac{\partial}{\partial Z} - \frac{\partial}{\partial R} \right). \end{aligned}$$

A developed form of the dispersion relation can be found in Menou et al. (2004). The Brunt-Väisälä frequency, N , which measures the magnitude of thermal stratification, comes out of the first bracket term in Eq. (6). Similarly, the epicyclic frequency, which measures the angular momentum “stratification,” comes out of the second bracket term. The notation is standard and identical to that adopted in Menou et al. (2004): \mathbf{v} is the fluid velocity, ρ is the mass density, P is the pressure, Φ is the gravitational potential, T is the temperature, \mathbf{B} is the magnetic field, μ is the dynamic viscosity, $\nu = \mu/\rho$ is the kinematic viscosity, η is the resistivity, χ is the heat conductivity and \mathbf{v}_A is the Alfvén speed.

A value $\gamma = 5/3$ is adopted for the gas adiabatic index and a perfect gas equation of state is assumed. The basic state rotation is given by $\boldsymbol{\Omega} = (0, 0, \Omega(R, Z))$ along the Z -axis. The basic state magnetic field, whose geometry is specified below, is assumed to be weak with respect to both rotation and thermal pressure.

2.2. Parameters for the Early Sun

For our early Sun study, we adopt conditions which correspond approximately to the zero-age main sequence Sun. Environmental parameters in the early Sun’s radiative zone which are important for our stability analysis include local values of the density and temperature, from which we determine the various diffusion coefficients, and the value of the Brunt-Väisälä frequency, which determines the magnitude of thermal stratification.

Tables 1 and 2 list the values of all the relevant parameters adopted in our stability survey, at two different radii in the radiative zone of the early Sun. Note that these radii ($r = 0.3$ and 0.7) are expressed in units of the early Sun’s radius, which is taken to be 0.87 times that of the current Sun (R_\odot). More generally, quantities with a solar symbol subscript refer to values for the current Sun. For instance, we consider a faster rotating early Sun, with an angular velocity $\Omega \geq \Omega_\odot \simeq 2.7 \times 10^{-6} \text{ rad s}^{-1}$. Values for the density, ρ , and temperature, T , in the radiative zone of the early Sun were estimated from Bahcall, Pinsonneault & Basu (2001). A standard opacity table was used to deduce the radiative opacity, κ . Values for

the kinematic viscosity, ν , radiative viscosity, ν_r , resistivity, η and radiative diffusivity, ξ_{rad} , were determined from standard relations for a fully ionized gas, as described in Menou et al. (2004). Finally, the value of the Brunt-Väisälä frequency, N , was estimated from the evolutionary models of Demarque & Guenther (1991).

A comparison between our Tables 1 & 2 and the corresponding Table 1 in Menou et al. (2004) reveals that conditions in the radiative zones of the early Sun and the current Sun are not very different from each other, from the point of view of our analysis. The ratio Ω_{\odot}^2/N^2 differs by a factor of a few in the two cases, and so does the Prandtl number, $\epsilon_{\nu} \equiv \nu/\xi_{rad}$, and the Acheson number, $\epsilon_{\eta} \equiv \eta/\xi_{rad}$. If anything, conditions are somewhat less double-diffusive in the early Sun (with larger values of ϵ_{ν} and ϵ_{η}) than in the current Sun. As we shall see, it is then mostly the possibility that the early Sun was rotating several times faster than it currently is which makes it particularly sensitive to diffusive rotational instabilities.

2.3. Numerical solutions

The dispersion relation (Eq. [6]) is of such complexity that it is difficult to derive from it general necessary and sufficient conditions for stability from it (Menou et al. 2004). In addition, we are interested here in studying the properties of unstable modes, not just the extent of stability domains. We thus solve the dispersion relation numerically, with a set of parameters appropriate for the early Sun (§2.2). This is done using the Laguerre algorithm described by Press et al. (1992) to solve Eq. (6) as a fifth-order complex polynomial for $\sigma = -i\omega$, with real coefficients.

It is useful to rewrite both the rotational and thermal stratification bracket terms appearing in the dispersion relation in spherical coordinates (r, θ, ϕ) . The thermal stratification term then becomes function of N^2 , θ and the radial and angular wavevectors, k_r and k_{θ} , for a spherically symmetric star. The rotational stratification term, on the other hand, explicitly depends on the amount of differential rotation within and across spherical shells, that we express as $\partial \ln \Omega / \partial \theta$ and $\partial \ln \Omega / \partial \ln r$, respectively. Here, we are interested in the specific case corresponding to $\partial \ln \Omega / \partial \theta = 0$ (no differential rotation within a spherical shell) but various degrees of negative differential rotation across spherical shells ($\partial \ln \Omega / \partial \ln r < 0$). This choice is dictated by the fact that weakly-magnetized radiative zones with any $\partial \ln \Omega / \partial \theta < 0$ are subject to the standard (adiabatic) magneto-rotational instability (Balbus & Hawley 1994). To explain the current solid body rotation of the Sun’s radiative zone, it is the more challenging $\partial \ln \Omega / \partial \ln r < 0$ case which is also most relevant, given the general expectation of faster rotating inner regions (§1).

We search for unstable modes (which correspond to σ -roots with positive real parts) at various locations on the sphere within the radiative zone. We consider values of the polar angle, θ , in the range $0 \rightarrow \pi/2$ (pole to equator). At each location, we perform a search for the fastest growing unstable mode by varying the wavevector components k_r and k_θ independently in the range $\pm[2\pi/l_{\max}, 2\pi/l_{\min}]$, on a 400×400 grid in k -space. The first, large-scale limit, l_{\max} , is chosen to be $\lesssim H \simeq \mathfrak{R}T/g$, the pressure scale height (where \mathfrak{R} is the perfect gas constant and g is the local gravitational acceleration). This guarantees that the local and weak field assumptions of our analysis remain valid. The second, small-scale limit, l_{\min} , is chosen to be $\gg \lambda$, the mean free path, so that the analysis remains valid given our use of fluid equations. The exact value adopted for λ turns out to be unimportant, as we find that all modes tend to be stabilized by diffusion on such extremely small spatial scales anyway.

It is generally difficult to guarantee that one has successfully identified, with a discrete search in k -space, the fastest growing mode for a given set of environmental parameters in the dispersion relation. However, we have performed extensive numerical convergence tests (at twice and four times the resolution in each dimension) which suggest that our results are indeed converged. At less than half the standard resolution adopted, on the other hand, deviations from our converged results start becoming significant. We find that the identification of fastest growing modes is facilitated (in terms of numerical resolution) as conditions become increasingly more unstable (e.g., an increased rate of differential rotation). Additional tests showing that our coding of the dispersion relation behaves as expected in various idealized limits have been described in Menou et al. (2004; see also Menou 2004). As mentioned in these studies, it is possible to verify explicitly the diffusive nature of unstable modes by imposing very small changes in the values of the diffusion coefficients and being able to witness small, but discernible effects on the mode properties. This is in contrast with the lack of such dependence in the case of adiabatic modes (which emerge, e.g., when $\partial \ln \Omega / \partial \theta < 0$).

2.4. Efficiency of Transport: “Turbulent Viscosity”

It is unclear whether one can determine, from a linear analysis only, the efficiency of transport that would result from non-linear growth and turbulence. We will adopt an often-used prescription here, by assuming that the efficiency of transport can be crudely estimated from the growth rate and the wavelength of the fastest-growing unstable linear mode. There is no general justification for this simple prescription, which may be off even at the order of magnitude level. Our goal here, however, is not to estimate too accurately the efficiency of

momentum transport between shells, but rather to determine whether, qualitatively, diffusive rotational instabilities could be responsible for angular momentum transport at the level required to affect globally a pattern of differential rotation in the Sun’s radiative zone.

It should be noted that the non-linear numerical simulations of Korycansky (1991) lend support to the simple prescription adopted here. This author found, for an equatorial setup (i.e. aligned thermal and angular momentum stratifications), that the non-linear behavior of hydrodynamical double-diffusive (GSF) modes is well described by a combination of linear growth rate and radial wavelength of the instability. Assuming this property carries over to magnetized modes and to other geometries (i.e. away from the stellar equator), we will be estimating the efficiency of angular momentum transport across spherical shells with the quantity $\sigma_{\max}/k_{r,\max}^2$ (dimension of a viscosity), where σ_{\max} is the growth rate of the fastest-growing mode and $k_{r,\max}$ is the spherical-radial wavevector component of that same mode. We will refer to this quantity as “turbulent viscosity” in what follows. Clearly, using linear theory to predict a non-linear outcome is a daring extrapolation, so one should treat our results on transport efficiencies with extreme caution.

With this caveat in mind, a global measure of the efficiency of angular momentum transport required in the Sun’s radiative zone is obtained from the minimum turbulent viscosity value needed to affect differential rotation on a characteristic timescale, τ . Choosing a billion years as a reference turbulent viscous time, one requires a turbulent viscosity

$$\nu_{\text{turb}} > \frac{R_{\odot}^2}{\tau = 10^9 \text{ years}} \sim 1.5 \times 10^5 \text{ cm}^2 \text{ s}^{-1}. \quad (7)$$

This minimum value of ν_{turb} will be useful in comparison to turbulent viscosity values estimated from our stability survey. Notice that this value is indeed several orders of magnitude larger than the values of the microscopic viscosities ν and ν_r listed in Table 1.

3. Results

In our analysis, the two main parameters determining the stability of the early Sun’s radiative zone are its angular velocity Ω ($\geq \Omega_{\odot}$) and the rate of negative differential rotation across spherical shells ($\partial \ln \Omega / \partial \ln r < 0$) assumed to be present. While one can safely assume that the Sun was not rotating much faster than 30-50 times its current rate in the past, it is much more difficult to estimate what level of radial differential rotation may have been present. Noting that the Keplerian shear rate, which is strong even by astronomical standards, would correspond to $\partial \ln \Omega / \partial \ln r = -3/2$ along the equator, we systematically survey the parameter space for values of $\partial \ln \Omega / \partial \ln r$ ranging from 0 to -2.5 . Independently, we vary the value of the local angular velocity Ω from Ω_{\odot} to $31 \Omega_{\odot}$.

Even with these choices, the number of free parameters in our stability analysis remains large. For simplicity, we focus in §3.1 and §3.2 on special cases, which turn out to be both illustrative and representative. They correspond to a specific choice of location/geometry in the early Sun ($r = 0.7$, $\theta = \pi/4$) and to specific magnetic field conditions ($B = 0$ or $B_\theta = 4$ G). We then discuss in §3.3 and §3.4 additional parameter dependencies as they emerged from our extended survey.

3.1. Fastest Growing GSF Modes

The dispersion relation (Eq. [6]) can be solved in the hydrodynamic limit ($v_A = \eta = 0$), in which case it reduces exactly to the dispersion relation of Goldreich & Schubert (1967). In this limit, we can thus examine the stability properties of the early Sun’s radiative zone with respect to GSF modes.

Figure 1 shows the growth rate, σ (in units of the angular velocity Ω ; left panel), and the corresponding “turbulent viscosity,” σ/k_r^2 (in units of $\text{cm}^2 \text{s}^{-1}$; right panel), of the fastest growing GSF mode, under early Sun conditions at $r = 0.7$ and $\theta = \pi/4$. In both panels, color contours of σ and σ/k_r^2 as a function of the assumed angular velocity, Ω/Ω_\odot (horizontal axis), and rate of negative differential rotation, $\partial \ln \Omega / \partial \ln r$ (vertical axis), are shown.

In an early Sun rotating at the same rate as the current Sun, GSF instabilities appear only for relatively strong rates of radial differential rotation. As the rotation rate is increased to a few times the current one, however, GSF instabilities are much more easily triggered, and for values of $\Omega/\Omega_\odot \gtrsim 5$ –10, any radial differential rotation stronger than $\partial \ln \Omega / \partial \ln r \lesssim -0.25$ is GSF-unstable. Notice how the growth rates, in units of Ω , become of order unity and independent of Ω/Ω_\odot for values of this parameter $\gtrsim 10$ –15.

It is remarkable that the current rotation rate of the Sun corresponds approximately to the stability limit for GSF modes (as shown by the sharp drop in contours as $\Omega/\Omega_\odot \rightarrow 1$ in Fig. 1). There is nothing that guarantees this a priori in our stability analysis. As we shall see later, this is related to a close equality between dynamical and diffusive timescales for current Sun conditions, a coincidence which was already commented upon by, e.g., Acheson (1978). We will revisit this issue in §4.

Despite their prominence in the faster-rotating early Sun, GSF modes may not have been able to provide efficient enough angular momentum transport to modify the existing differential rotation rate. As shown in the right panel of Fig. 1, turbulent viscosities associated with fastest growing GSF modes tend to be small: $\nu_{\text{turb}} \sim 10^{1-4} \text{ cm}^2 \text{ s}^{-1}$. According to Eq. (7), this is not sufficient to provide much transport over the 5 billion years lifetime of

the Sun. Another limitation of GSF modes, as we have already mentioned, is that they are not expected to bring the fluid to a state of solid body rotation (at marginal stability). This is in contrast with the MHD versions of these diffusive modes, which have the potential to lead to solid body rotation (at marginal stability; Menou et al. 2004).

3.2. Fastest Growing MHD Modes

Figure 2 shows growth rate and turbulent viscosity values obtained for the fastest growing MHD modes in the presence of a purely polar magnetic field of strength $B_\theta = 4$ G, for the same early Sun conditions at $r = 0.7$ and $\theta = \pi/4$ as before. While the contour plots are broadly consistent with those in Fig. 1, important quantitative differences emerge. The MHD nature of the fastest growing modes under these conditions can be verified by changing slightly the magnetic field strength and being able to witness small, but discernible effects on the mode properties (see also our discussion of the effects of magnetic field strength in §3.3).

Fastest growing MHD modes which have very slow growth rates have been voluntarily truncated from the σ contour plot (left panel, Fig. 2), for values of $\sigma/\Omega < 0.01$. This greatly facilitates the identification of regions which are only marginally unstable, by comparison with the corresponding contours of turbulent viscosity in the right panel of Fig. 2 (which include all fastest growing modes, no matter how slowly they are growing). It is clear from this comparison of the two panels in Fig. 2 that substantial regions of the parameter space surveyed for MHD modes correspond to fastest growing modes which are in fact growing quite slowly. Contrary to GSF modes (Fig. 1), only for the largest values of Ω/Ω_\odot and $\partial \ln \Omega / \partial \ln r$ do the growth rates, σ/Ω , approach unity for MHD modes. Note also that unstable MHD modes only appear for values of $\Omega/\Omega_\odot \gtrsim 3-4$. This leads us to conclude that, in the presence of a magnetic field, it is more difficult to trigger diffusive rotational instabilities (for the conditions in the early Sun’s radiative zone).

This difficulty comes with an attractive feature, however, from the point of view of transport. As the right panel of Fig. 2 shows, fastest growing MHD modes tend to have larger associated turbulent viscosity values than their hydrodynamic GSF counterparts, by orders of magnitude (compare right panel of Fig. 1). Even though fastest growing MHD modes tend to grow more slowly than GSF modes, they do so on larger scales than the corresponding fastest growing GSF modes, which results in an effectively larger turbulent viscosity estimate for the MHD case (at least according to our extrapolation from linear theory).

This difference between MHD and hydro (GSF) modes can be understood simply as being a consequence of the destabilizing role played by magnetic tension in MHD modes. Our diffusive MHD modes are intrinsically magneto-rotational in nature. The role of magnetic tension for the magneto-rotational instability has been documented extensively (e.g. Balbus & Hawley 1998). It is well known that, for a given magnetic field strength and orientation, magnetic tension picks a specific “most unstable” scale, below which it ultimately acts as a stabilizing agent (i.e. like a slow MHD wave) and above which it becomes very inefficient at destabilizing the flow. Provided that this best scale for destabilizing magnetic tension is much larger than the diffusive scales in the problem, one would expect rather slowly growing MHD modes (since diffusion, slower on larger scales, is still necessary for any instability), operating on larger scales than their hydrodynamical (GSF) counterparts. This interpretation is consistent with all our survey results for fastest growing MHD and GSF modes.

3.3. Dependence on the Magnetic Field Strength

One would also expect the hydrodynamic nature of the fastest growing modes to be recovered for small enough values of the magnetic field strength, when the “most unstable” scale picked by magnetic tension becomes comparable to the typical diffusive scales associated with GSF modes. We indeed observe such a hydro-to-MHD transition in our parameter space survey.

Figure 3 shows how the properties of the fastest growing mode are affected by changes in the assumed strength of the magnetic field. For ease of comparison, the same early Sun conditions as before, at $r = 0.7$ and $\theta = \pi/4$, have been adopted here as well. Furthermore, the local rates of rotation and radial differential rotation have been fixed to $\Omega/\Omega_{\odot} = 20$ and $\partial \ln \Omega / \partial \ln r = -1$. We are thus effectively looking at a single point in the contour plots of Fig. 1 and 2 and studying how the transition from the hydrodynamic to the MHD regime proceeds as the magnetic field strength is varied. Figure 3 shows how this transition happens for a purely radial field ($B_r = 10^{-3.5} - 10^{+2.5}$ G; dashed lines) and a purely polar field ($B_{\theta} = 10^{-3.5} - 10^{+2.5}$ G; solid lines). The effects of the hydro-to-MHD transition are monitored in terms of the same normalized growth rate, σ/Ω (left panel), and turbulent viscosity, σ/k_r^2 (right panel), for the fastest growing mode as before.

For low enough values of the magnetic field ($B_r, B_{\theta} \ll 0.1$ G), the fastest growing mode properties become independent of the magnetic field strength and one verifies that the results for purely hydrodynamic GSF modes are indeed recovered. As the value of B is increased beyond 0.1 G, the first effect is a reduction in the growth rate of the most unstable mode, followed quickly by an increase for $B \gtrsim 0.5$ G. From then on, the effect of increasing

B depends on the field geometry. A larger field tends to lead to faster growing MHD modes and to larger values of the turbulent viscosity (as measured by σ/k_r^2). Although this trend ends and reverses in the case of the strictly polar field (solid line), for $B_\theta \gtrsim 1$ G, we shall see below, when we discuss Fig. 4, that this change of behavior is mostly an artifact of our method, which signals the breakdown of the local theory adopted.

A key feature of the transition from hydro to MHD diffusive modes is the increase in the turbulent viscosity value (σ/k_r^2). The horizontal dash-dotted line in the right panel of Fig. 3 indicates the minimum value of ν_{turb} required for global transport in the Sun’s radiative zone on a timescale $\sim 10^9$ yr (Eq. [7]). While the turbulent viscosity that we estimate for hydro GSF modes seems insufficient to have had an effect on the internal rotation profile of the early Sun’s radiative zone, diffusive modes in the MHD regime ($B \gg 0.1$ G) are apparently capable of transporting angular momentum efficiently enough.

Figure 4 illustrates two additional properties of these fastest growing unstable modes as they make the transition from hydro to MHD (same notation as in Fig. 3). The ratio of their radial to polar wavenumbers is shown in the left panel, while the ratio of their radial wavelength to the local pressure scale height is shown in the right panel. Fastest growing hydro (GSF) modes tend to have comparable radial and polar wavenumbers, while MHD modes have predominantly polar wavenumbers (and thus polar wavevectors, which correspond to predominantly radial displacements). In addition, while hydro GSF modes are confined to rather small spatial scales relative to the local pressure scale height ($k_H/k_r \ll 1$), fastest growing MHD modes have increasingly larger radial wavelengths as the magnetic field strength is increased, as expected if the spatial scale favored by the destabilizing magnetic tension is forced to larger scales by the stronger magnetic field.

As explained in §2.3, we have voluntarily limited our search for fastest growing unstable modes to wavelengths smaller than the local pressure scale height. This limit is manifestly reached in the case of large enough polar field strengths (solid line in the right panel of Fig. 4) and, retrospectively, it is clear that this limit being reached affects all the other properties shown in Figs. 3 and 4 for this specific field geometry (when $B_\theta \gtrsim 1$ G). Although this may signal the breakdown of the local stability theory used, it is clear from the trends in Figs. 3 and 4 that extrapolations beyond the local limit would tend to reinforce our main conclusions: fastest growing diffusive MHD modes have larger wavelengths and appear to be more efficient at transporting angular momentum across spherical shells than their hydrodynamical (GSF) counterparts.

3.4. Other Parameter Dependencies

We have verified that the trends illustrated in Figs. 1–4 remain generally valid throughout the parameter space surveyed. We have varied the geometry of the stability problem by picking values of θ from 0 to $\pi/2$. While rotational instabilities tend to be somewhat favored (or stronger) at $\theta = \pi/2$ (equator), the difference with the $\theta = \pi/4$ is small. As $\theta \rightarrow 0$ (pole), rotational instabilities relying on radial differential rotation are disfavored, as one expects from simple geometrical considerations. This points to a general asymmetry in transport between equatorial and polar regions, but we have not explored this trend more systematically.

We have also explored stability at a different location, $r = 0.3$, in the early Sun’s radiative zone. As expected from the scalings in Tables 1 and 2, conditions are less double-diffusive (and thus less prone to instability) at this radius than at $r = 0.7$. For $r = 0.3$, we find growth rate and turbulent viscosity contours which are roughly consistent with those shown in Figs. 1 and 2, except that they are all shifted to larger values of Ω/Ω_\odot , by a factor 4–5. For instance, GSF modes do not appear in our survey at $r = 0.3$ before values of $\Omega \gtrsim 5\Omega_\odot$ (vs. $\Omega \simeq \Omega_\odot$ in Fig. 1). Similarly, for the same MHD conditions as in Fig. 2, values of $\Omega/\Omega_\odot \gtrsim 15$ –20 are required to trigger instability at a rate of differential rotation $\partial \ln \Omega / \partial \ln r = -1$, and values of $\Omega/\Omega_\odot \gtrsim 30$ are required for instability if $\partial \ln \Omega / \partial \ln r = -0.5$. In all aspects except these changes in the location of the stability domains, our results for $r = 0.3$ are comparable to those at $r = 0.7$.

4. Discussion and Conclusion

The main conclusions of our stability survey for the early Sun’s radiative zone can be summarized as follows. Provided that the early Sun was rotating at least a few times faster than it currently is, we find that it was easily subject to diffusive hydro- and magneto-rotational instabilities. That is, rather weak levels of negative radial differential rotation (across spherical shells) were sufficient to trigger these linear instabilities. This result complements the one stating that any level of negative differential rotation within a spherical shell ($\partial \ln \Omega / \partial \theta < 0$) triggers the standard (adiabatic) magneto-rotational instability within that shell (Balbus & Hawley 1994). An inspection of our survey results suggests that diffusive magneto-rotational instabilities may be more efficient at transporting angular momentum than their hydrodynamical (GSF) counterparts because fastest growing unstable modes typically have larger wavelengths in the magnetized case. A simple interpretation of this trend in terms of the scale favored by a destabilizing magnetic tension was offered. This leads us to conclude that diffusive magneto-rotational instabilities are attractive candidates to ex-

plain the angular momentum transport (and possibly the elemental mixing) that must have occurred in the Sun’s radiative zone.

Additional work will be required to establish these promising trends on firmer grounds. Indeed, a number of questions raised by our investigation remain unanswered at this point. Chief among them is the issue of the primordial strength (and to some extent geometry) of the magnetic field present in the Sun’s radiative zone. Our study of the hydro-to-MHD transition shows that if the magnetic field initially present in the Sun’s radiative zone was too weak, the fluid would have behaved largely as if it were unmagnetized, as far as rotational instabilities are concerned.² The minimum magnetic field values needed for the fluid stability to be determined by MHD processes are not large ($B \gtrsim 0.1$ G) and they do not violate current upper limits on the field strength in the Sun’s radiative zone (e.g. Friedland & Gruzinov 2004 and references therein). However, if the Sun’s radiative zone was initially seeded with only a very weak magnetic field, the growth of GSF instabilities would be favored and the resulting transport may then be weak. Diffusive magneto-rotational instabilities could eventually play a role if these GSF instabilities were able to grow the background seed field to a large enough value for MHD modes to take over. Although this hypothetical scenario shares some similarities with the kinematic dynamo problem, the likelihood of its success remains very unclear at this point.

In addition to this dependence on seed field conditions, the role of diffusive rotational instabilities is likely to be affected by the chemical structure and evolution of the radiative zone in which they operate. By analogy with the result of Goldreich & Schubert (1967) on the strongly stabilizing role of composition gradients, one would generally expect diffusive rotational instabilities to be quenched when substantial composition gradients start developing in a radiative zone. This may limit to very early times only their role for the innermost radiative core of the Sun and it points, more generally, to the possibility of a complex, coupled chemical-rotational evolution (since turbulent mixing could affect the magnitude of the stabilizing composition gradients being established). In regions where composition gradients end up being significant (like the current Sun inner radiative core), it appears likely that the dynamo and transport process advocated by Spruit (2002) and simulated by Braithwaite & Spruit (2006) would be dominant and free to operate (see also Heger, Woosley & Spruit 2005 for an application to massive star evolution). In regions with negligibly small composition gradients, however, diffusive modes, growing exponentially with time constants approaching

²We note that there is a well-known pathology if one attempts to recover the stability conditions of an unmagnetized fluid by taking the zero-field limit of the corresponding ideal MHD stability conditions (e.g. Balbus 1995). Our results are interesting in this respect, as they show how the proper unmagnetized limit can be recovered at small, but finite, field values, when diffusive effects are properly accounted for.

the local value of the angular velocity (Figs. 1 and 2), are likely to dominate over a linear growth by field stretching, which is invoked in the initial phase of the scenario proposed by Spruit (2002; see also Braithwaite & Spruit 2006).

Let us conclude by mentioning that the locations of stability domains, as found in our survey, are broadly consistent with a simple argument involving a balance between local diffusive and dynamical timescales. Acheson (1978) already emphasized that instability to double-diffusive GSF modes should be approximately determined by the criterion

$$\frac{\nu}{\xi} \lesssim -\frac{\kappa^2}{N^2}, \quad (8)$$

where κ is the epicyclic frequency (which must be imaginary for instability). This simply states that the stabilizing role of thermal stratification (N^2) must be neutralized by a strong enough heat diffusivity (ξ), but that at the same time the destabilizing role of the angular momentum profile ($\kappa^2 < 0$) must not be neutralized by momentum diffusion (i.e. viscosity, ν). This simple criterion appears to be approximately satisfied in our stability survey. Similarly, our survey results indicate that instability to double-diffusive MHD modes is roughly determined by a similar criterion,

$$\frac{\eta}{\xi} \lesssim -\frac{\partial\Omega^2/\partial \ln r}{N^2}, \quad (9)$$

where η is the resistivity. This explains why unstable MHD modes only appear for values of Ω/Ω_\odot which are a few times larger than for GSF modes, in approximate proportion with the ratio $\sqrt{\eta/\nu}$. It would be interesting to apply these simple criteria to the radiative zones of other stars than the Sun, at different stages of their evolution, to determine more generally how relevant diffusive rotational instabilities may be for the evolution of rotating stars.

REFERENCES

- Acheson, D. J. 1978, *Phil. Trans. Roy. Soc. London*, 289A, 459
- Bahcall, J. N., Pinsonneault, M. H. & Basu, S. 2001, *ApJ*, 555, 990
- Balbus, S. A. & Hawley, J. F. 1994, *MNRAS*, 266, 769
- Balbus, S. A., & Hawley, J. F. 1998, *Rev. Mod. Phys.*, 70, 1
- Balbus, S. A. 1995, *ApJ*, 453, 380
- Braithwaite, J. & Spruit, H.C. 2006, *A&A submitted*, astro-ph/0509693

- Chaboyer, B., Demarque, P. & Pinsonneault, M. H. 1995a, *ApJ*, 441, 865
- Chaboyer, B., Demarque, P. & Pinsonneault, M. H. 1995b, *ApJ*, 441, 876
- Charbonnel, C. & Talon, S. 2005, *Science*, 309, 2189
- Demarque, P. & Guenther, D. B. 1991, in *Solar Interior and Atmosphere*, eds. A.N. Cox, W.C. Livingston and M.S. Matthews (Tucson: University of Arizona Press), p. 1186
- Eggenberger, P., Maeder, A. & Meynet, G. 2006, *A&A* in press, astro-ph/0508455
- Fricke, K. 1968, *Z. Ap.*, 68, 137
- Friedland, A. & Gruzinov, A. 2004, *ApJ*, 601, 570
- Garcia-Lopez R. J., Spruit H., 1991, *ApJ*, 377, 268
- Goldreich, P. & Schubert, G. 1967, *ApJ*, 150, 571
- Heger, A., Woosley, S. E. & Spruit, H. C. 2005, *ApJ*, 626, 350
- Korycansky, D. G. 1991, *ApJ*, 381, 515
- Kumar, P. & Quataert, E. 1997, *ApJ*, 475, L143
- MacFadyen, A. I. & Woosley, S. E. 1999, *ApJ*, 524, 262
- Mathis, S. & Zahn, J.-P. 2005, *A&A*, 440, 653
- Menou, K. 2004, *MNRAS*, 352, 1381
- Menou, K., Balbus, S. A. & Spruit, H. C. 2004, *ApJ*, 607, 564
- Ott, C. D., Burrows, A., Thompson, T. A., Livne, E. & Walder, R. 2006, *ApJ* in press, astro-ph/0508462
- Press W. H., 1981, *ApJ*, 245, 286
- Press, W. H., Teukolsky, S. A., Vetterling, W.T. & Flannery, B. P. 1992, *Numerical Recipes in Fortran. The art of scientific computing* (Cambridge: Cambridge University Press)
- Rashba, T. I., Semikoz, V. B. & Valle, J. W. F. 2005, Technical note IFIC/05-62, MPP-2005-151, astro-ph/0511708
- Rogers, T. M. & Glatzmaier, G. A. 2005, *MNRAS*, 364, 1135

- Rogers, T. M. & Glatzmaier, G. A. 2006, ApJ submitted, astro-ph/0511739
- Sofia, S., Kawaler, S., Larson, R. & Pinsonneault, M. 1991, in Solar Interior and Atmosphere, eds. A.N. Cox, W.C. Livingston and M.S. Matthews (Tucson: University of Arizona Press), p. 140
- Schatzman, E. 1991, in Solar Interior and Atmosphere, eds. A.N. Cox, W.C. Livingston and M.S. Matthews (Tucson: University of Arizona Press), p. 192
- Schatzman E., 1993, A&A, 279, 431
- Spruit, H. C. 2002, A&A, 381, 923
- Talon, S. & Zahn, J.-P. 1998, A&A, 329, 315
- Talon, S., Kumar, P. & Zahn, J.-P. 2002, ApJ, 574, L175
- Tassoul, J.-L. 1978, Theory of Rotating Stars (Princeton: Princeton University Press)
- Thompson, M. J., Christensen-Dalsgaard, J., Miesch, M. S. & Toomre, J. 2003, ARA&A, 41, 599
- Turck-Chieze, S. et al. 2005, in Proceedings of 2005 ESLAB symposium 19-21 April 2005, astro-ph/0510854
- Woosley, S. E., Heger, A. & Weaver, T. A. 2002, Rev. Mod. Phys. 74, 1015
- Zahn, J.-P. 1974, in Stellar Instability and Evolution, Proc. IAU Symp. 129, eds. P. Ledoux, A. Noels and A.W. Rodgers (Dordrecht: D. Reidel), p. 185

Table 1: Conditions in the Early Sun’s Radiative Zone

Radius ($0.87 R_{\odot}$)	ρ (g cm^{-3})	T (10^6 K)	κ ($\text{cm}^2 \text{ g}^{-1}$)	ν ($\text{cm}^2 \text{ s}^{-1}$)	ν_r ($\text{cm}^2 \text{ s}^{-1}$)	η ($\text{cm}^2 \text{ s}^{-1}$)	ξ_{rad} ($\text{cm}^2 \text{ s}^{-1}$)
$r \simeq 0.7$	0.4	2.6	20	15	1	496	4×10^6
$r \simeq 0.3$	20	7	3.5	3.5	0.1	112	1.8×10^5

Table 2: Conditions Relevant to Diffusive Stability in the Early Sun’s Radiative Zone

Radius ($0.87 R_{\odot}$)	N^2 (Hz^2)	Ω_{\odot}^2/N^2	ϵ_{ν}	ϵ_{η}
$r \simeq 0.7$	6×10^{-6}	1.2×10^{-6}	4×10^{-6}	1.2×10^{-4}
$r \simeq 0.3$	6×10^{-6}	1.2×10^{-6}	2×10^{-5}	6.2×10^{-4}

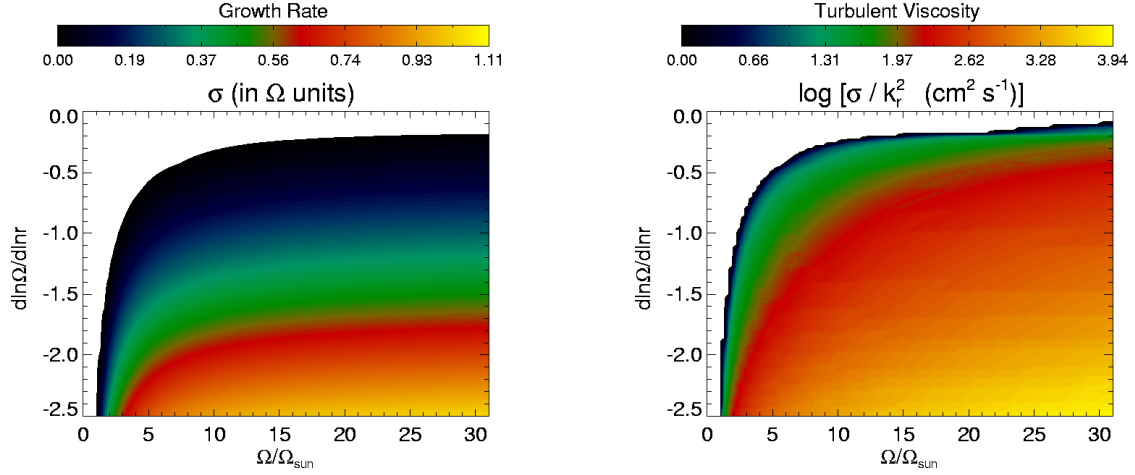


Fig. 1.— Growth rate (left, σ/Ω) and “turbulent viscosity” (right, σ/k_r^2) of fastest growing hydrodynamical (“GSF”) modes, as a function of the rotation rate ($\Omega/\Omega_{\text{sun}}$) and the level of differential rotation across spherical shells ($d \ln \Omega / d \ln r$). The stability survey is performed at a specific location in the early Sun’s radiative zone, corresponding to a polar angle $\theta = \pi/4$ and a spherical radius $r = 0.7$ (in units of the early Sun radius, see Table 1).

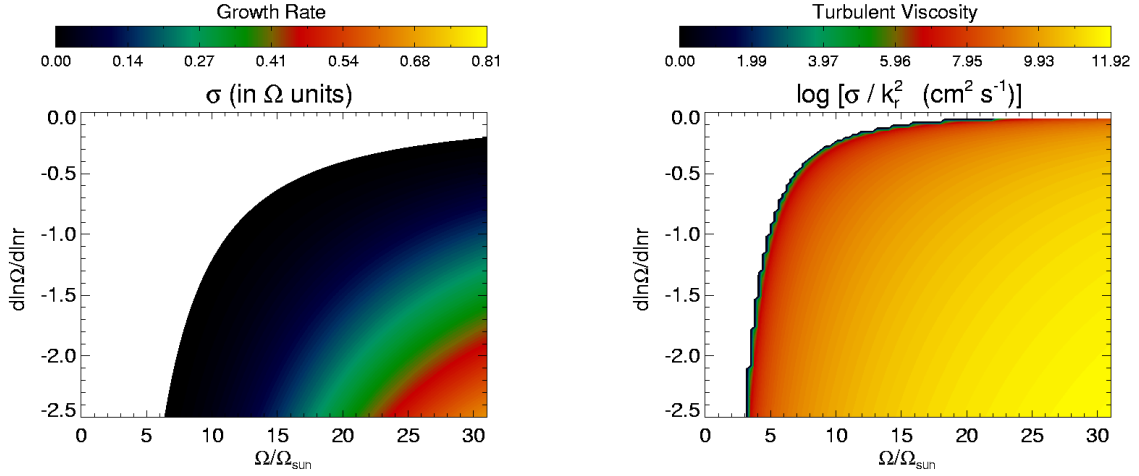


Fig. 2.— Growth rate (left, σ/Ω) and “turbulent viscosity” (right, σ/k_r^2) of fastest growing MHD modes, as a function of the rotation rate ($\Omega/\Omega_{\text{sun}}$) and the level of differential rotation across spherical shells ($d\ln\Omega/d\ln r$). The stability survey is performed at a specific location in the early Sun’s radiative zone, corresponding to a polar angle $\theta = \pi/4$ and a spherical radius $r = 0.7$ (in units of the early Sun radius), and for a specific strength and geometry of the local magnetic field (polar field $B_\theta = 4$ G). Note that the linear color scale in the left panel truncates modes growing at a rate σ slower than 0.01Ω .

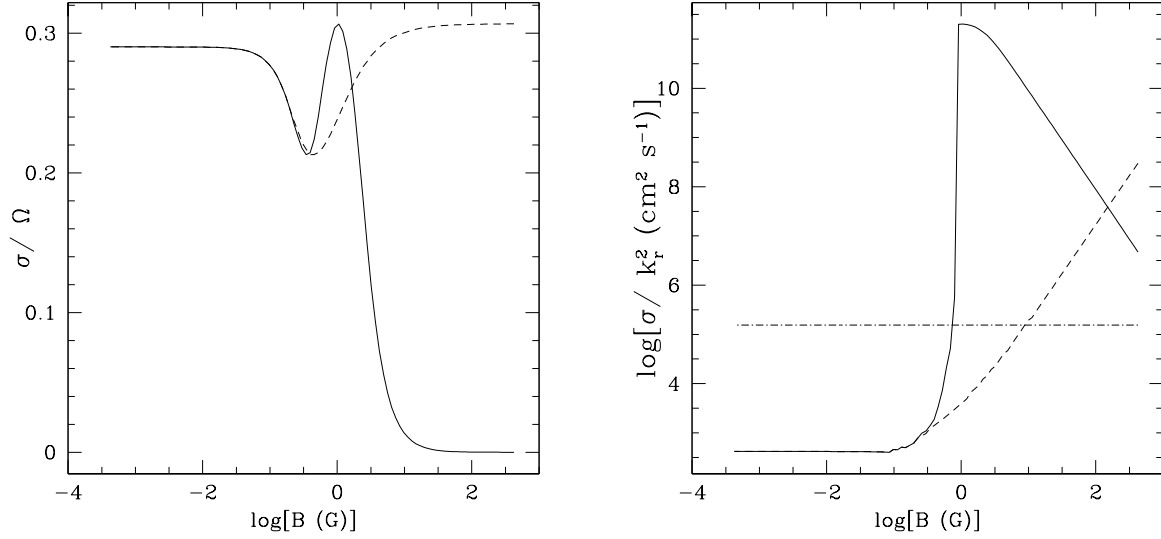


Fig. 3.— Growth rate (left, σ/Ω) and “turbulent viscosity” (right, σ/k_r^2) of the fastest growing mode, as a function of the strength and geometry of the magnetic field, B . Solid lines are for a purely polar field (B_θ only) and dashed lines for a purely radial field (B_r only). A rotation rate $\Omega = 20 \Omega_{\text{sun}}$ and a rate of differential rotation across spherical shells $d \ln \Omega / d \ln r = -1$ were assumed. The analysis is performed at a specific location in the early Sun’s radiative zone, corresponding to a polar angle $\theta = \pi/4$ and a spherical radius $r = 0.7$ (in units of the early Sun radius). Hydrodynamical GSF modes are recovered at low enough values of the magnetic field strength. The horizontal dash-dotted line in the right panel indicates the angular momentum transport efficiency required for a global transport timescale in the Sun $\sim 10^9$ yr.

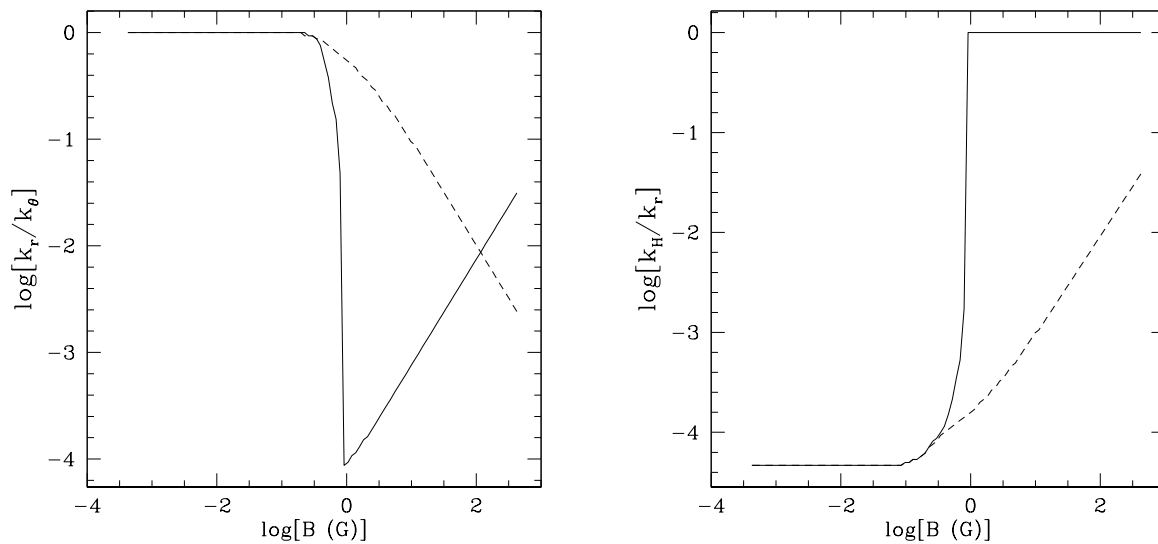


Fig. 4.— Ratio of radial to polar wavenumbers (left) and radial wavelength to local scale height (right) for the same unstable modes as shown in Fig. 3. MHD modes (at large B values) have preferentially radial displacements, with relatively large radial wavelengths (reaching the local scale height limit in the polar field case – solid line). Hydrodynamical modes (at low B values) have much smaller wavelengths.